Journal of Sound and Vibration (2002) **250**(5), 835–848
doi:10.1006/jsvi.2001.3976, available online at http://www.idealibrary.com on IDEAL®

DYNAMIC STABILITY OF STEPPED BEAMS UNDER MOVING LOADS

O. J. Aldraihem

Mechanical Engineering Department, King Saud University, P.O. Box 800, *Riyadh* 11421, *Kingdom of Saudi Arabia. E-mail: odraihem@ksu.edu.sa*

AND

A. Baz

Mechanical Engineering Department, University of Maryland, College Park, MD 20742, *U.S.A. E-mail: baz@eng.umd.edu*

(*Received* 12 *February* 2001, *and in final form* 16 *July* 2001)

The dynamic stability of a stepped beam subjected to a moving mass is investigated in this study. The equations of motion for transverse vibrations of the beam are developed in distributed parameter and finite element forms. The impulsive parametric excitation theory is used to predict the stability of the beam when subjected to periodic parametric excitations. The accuracy of the theory is verified by obtaining the stability boundaries of a simply supported beam and comparing the results with the results reported in the literature. Stability maps are then obtained for clamped–free uniform beams as well as clamped–free stepped beams. It is found that the stability of certain beam modes can be improved by providing the beam with appropriately spaced steps. It is shown that better stability characteristics can be obtained by using piezoelectric actuators. Stability analyses of beams with periodic piezoelectric and/or viscoelastic steps are a natural extension of the present work.

1. INTRODUCTION

A wide variety of beam-like structures are subjected to moving loads. Examples of these structures include bridges, fluid pipes, gun barrels, rails, and work pieces on machine tools. The dynamic behavior of this class of structures is quantified by considering their dynamic response and/or dynamic stability. In the dynamic response analyses, the system behavior is determined in the time and/or frequency domain. The analyses of dynamic stability involve, however, the computation of the boundaries between the stable and unstable regions. This is usually achieved by constructing the stability maps in the appropriate planes of system parameters.

The equations governing the dynamics of beams under moving loads have periodically time-varying coefficients resulting in the well-known class of parametrically excited vibrations. Considerable research effort has been put forth in studying the dynamic response of such a class of structural vibrations [1–12]. However, investigation of the dynamic stability has been limited only to a few classes of uniform beams [13–18]. The reason for such a limitation is due to the fact that the techniques used to study the stability

0022-460X/02/100835 + 14 $35.00/0

were based on the Mathieu–Hill method which cannot be easily employed for non-uniform beams with general boundary conditions. The Mathieu–Hill method was successfully utilized to provide approximate stability characteristics of the system [19, 20]. However, application of the method becomes difficult when the parametric excitation is not simple harmonic in time.

The studies of the dynamic stability of beams under moving loads include the work of Katz *et al.* [13], Benedetti [14], Nelson and Conover [15], Housner [16], Gregory and Paidoussis [17, 18]. For example, Housner [16] studied the dynamic stability of uniform pipes supported at both ends and conveying fluids. The work of Gregory and Paidoussis [17, 18] focused on obtaining the stability conditions of uniform cantilever pipes. Nelson and Conover [15] studied the dynamic stability of a simply supported uniform beam carrying a continuous series of mass particles using Floquet theory and the approximate Galerkin's method. Benedetti [14] extended the work of Nelson and Conover in order to predict the stability maps of a simply supported uniform beam using the Mathieu–Hill method. Katz *et al.* [13] investigated the dynamic stability of a uniform beam with simply supported ends. The beam was subjected to a moving concentrated force that was deflection-dependent. The stability regions were predicted by using the Mathieu–Hill method along with the Galerkin's method. It is important here to note that none of the previous studies, however, considered the dynamic stability of non-prismatic beams subjected to moving loads.

In the present study, the objective is to investigate the dynamic stability of stepped beams carrying masses. The stepped beam equations of motion are developed in two forms; namely, a discrete parameter form and a finite element form. In order to study the stability of the system, the impulsive parametric excitation method is used [20]. The stability of a simply supported uniform beam is obtained and the results are compared with the results available in the literature. The stability maps are then obtained for uniform and stepped beams with clamped–free boundary conditions.

2. THEORY AND FORMULATION

The system under consideration consists of a stepped beam of length L carrying a moving particle of mass m_v travelling with an axial velocity V, which is invariant with time (Figure 1). The beam's x-axis is assumed to pass through the centroid of the cross-section and to vibrate in the x–z plane.

The main assumptions for the beam and the moving mass are as follows: (1) the beam is symmetric and obeys the Euler–Bernoulli theory; (2) the steps can be made of passive solids, "viscoelastic" materials, and/or active "piezoelectric" materials; (3) the beam along with the

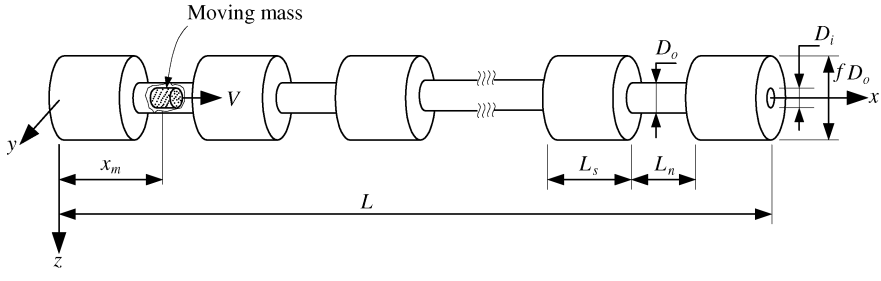

Figure 1. Stepped beam carrying moving mass.

steps have isotropic properties and are perfectly bounded to each other; (4) the moving mass does not generate friction force and is always in contact with the beam.

2.1. VARIATIONAL FORMULATION

The beam equations of motion along with the associated boundary conditions can be derived by using the extended Hamilton's principle which is defined as

$$\int_{t_1}^{t_2} [\delta(T - U) + \delta W_{nc}] \mathrm{d}t = 0, \tag{1}$$

where δ is the first variation, T is the system kinetic energy, U is the beam strain energy, and δW_{nc} is the virtual work done by the non-conservative forces (which includes structural damping and forces not accounted for in U). If the beam were to carry a continuous sequence of moving mass, δW_{nc} must include the mass discharge energy [21]. This is, in particular, important when one or both of the beam boundaries are free.

2.1.1. *Kinetic energy*

The kinetic energy of the beam system is the sum of the kinetic energy of the stepped beam, T_b, plus the kinetic energy of the moving mass, T_m. The kinetic energy attributed to the stepped beam is given by

$$T_b = \frac{1}{2}\int_0^L \rho A(\dot{w})^2 \mathrm{d}x, \tag{2}$$

where ρ is the beam mass density, A is the beam cross-sectional area and w is the transverse displacement of the beam.

The kinetic energy of the moving mass is

$$T_m = \tfrac{1}{2} m_v[v_z^2(x = x_m) + v_x^2(x = x_m)]. \tag{3}$$

Although the moving mass velocity relative to the beam is a constant V, the components of the absolute particle velocity vary with time and are given by

$$v_z = \dot{w} + Vw', \quad v_x = V(1 - \tfrac{1}{2}(w')^2) - \dot{u}, \tag{4}$$

with the primes denoting spatial derivative with respect to x and $\dot{u}$ defines the beam velocity in the x direction.

From equations (3, 4) and neglecting the higher order terms (i.e., approximate to second order), the kinetic energy of the moving mass reduces to

$$T_m = \tfrac{1}{2} m_v[\dot{w}^2 + 2V\dot{w}w' + V^2 - 2\dot{u}V]_{x=x_m}. \tag{5}$$

Hence, the total kinetic energy is obtained as

$$T = \frac{1}{2}\int_0^L \rho A(\dot{w})^2 \mathrm{d}x + \frac{1}{2} m_v[\dot{w}^2 + 2V\dot{w}w' + V^2 - 2\dot{u}V]_{x=x_m}. \tag{6}$$

2.1.2. *Strain energy*

When the steps are provided with piezoelectric capabilities, the piezoelectric strain should be included in the expression of the strain energy in order to satisfy its definition and

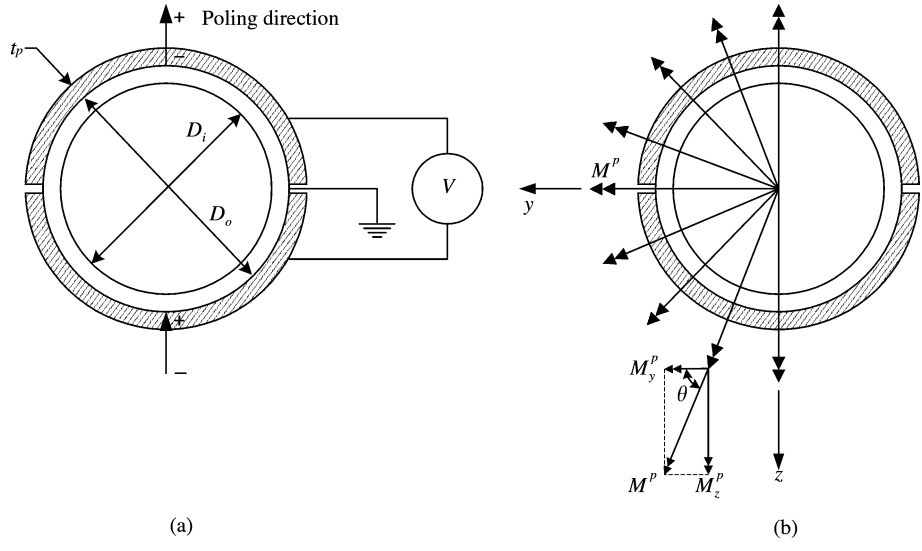

Figure 2. (a) Beam cross-section, (b) distributed resultant moment.

properties (i.e., positive definite and path independent). The strain energy of a beam with piezoelectric steps can be expressed as

$$U = \frac{1}{2}\int_0^L [EI(w'')^2 + 2M_y^P w'']\mathrm{d}x - (m_v \mathbf{g})w(x = x_m) + H_\mathrm{T} \tag{7}$$

and with reference to Figure 2, the y-component of the piezoelectric moment is defined by

$$M_y^P = \iint_A E\varepsilon_x^P z\cos\theta \mathrm{d}A,$$

where E denotes the Young's modulus, I denotes the beam moment of inertia, ε_x^P denotes the axial piezoelectric strain and H_T denotes a constant term, which will vanish with the first variation. Also, $\mathbf{g}$ denotes the gravitational acceleration.

2.1.3. *Work by non-conservative forces*

The work done by the non-conservative forces is only due to the internal damping of the beam. In this study, the damping is assumed to follow the Kelvin–Voigt model yielding [22]

$$\delta W_{nc} = -\int_0^L \eta I\dot{w}''\delta w''\mathrm{d}x, \tag{8}$$

where η is the damping coefficient.

2.2. DISTRIBUTED-PARAMETER MODEL

Using equation (1) with equations (6)–(8) and performing some manipulations, yields the equation of motion

$$\rho A\ddot{w} + EIw'''' = p_m(x,t) + p_d(x,t) + p_p(x,t), \tag{9a}$$

where

$$p_m(x,t) = -m_v[(\ddot{w} - g) + 2V\dot{w}' + V^2w'']_{x=x_m}[\delta(x - x_m)], \tag{9b}$$

$$p_d(x,t) = -\eta I\dot{w}'''', \quad p_p(x,t) = -(M_y^P)'' \tag{9c, d}$$

with boundary conditions at $x = 0$ and L

$$w \text{ specified or } \eta I\dot{w}''' + EIw''' = -m_vV[\dot{w} + Vw']_{x=x_m}[\delta(x - x_m)] - (M_y^P)' \tag{10}$$

and

$$w' \text{ specified or } \eta I\dot{w}'' + EIw'' = -M_y^P,$$

where $[\delta(x)]$ is the Dirac delta function.

Starting from the equality sign, the various terms on the right-hand side of equation (9b) may be identified, sequentially, as the moving mass inertia term, the Coriolis term, a centrifugal term. Although the Coriolis term contains a first derivative with respect to time, its influence is not the same as a viscous damping term. This will be clearly demonstrated when the system equations are presented by the discrete form.

2.3. FINITE ELEMENT MODEL

A one-dimensional beam element will be formulated to discretize the system equations. The shape functions used to approximate the transverse displacement are chosen to be Hermite cubic polynomials. The displacements of the beam elements are approximated by

$$w(x,t) = \sum_{i=1}^{4} N_i(x)v_i(t), \tag{11}$$

where v_1, v_2 (v_3 , v_4) are transverse displacement and rotation at the left (right) end of the finite element, and N_i are the shape functions given by

$$[\mathbf{N}]^T = \begin{bmatrix} 1 - 3\left(\dfrac{x - x_i}{h}\right)^2 + 2\left(\dfrac{x - x_i}{h}\right)^3 \\ (x - x_i) - 2h\left(\dfrac{x - x_i}{h}\right)^2 + h\left(\dfrac{x - x_i}{h}\right)^3 \\ 3\left(\dfrac{x - x_i}{h}\right)^2 - 2\left(\dfrac{x - x_i}{h}\right)^3 \\ -h\left(\dfrac{x - x_i}{h}\right)^2 + h\left(\dfrac{x - x_i}{h}\right)^3 \end{bmatrix}, \tag{12}$$

where x denotes the beam global x-co-ordinate, x_i denotes the distance from the left end of the beam to the left node of the ith finite element, and h denotes the length of the finite element.

Substitution of equation (11) into the extended Hamilton's principle (1) and integration over the spatial domains leads to a system of linear differential equations

$$([\mathbf{M}] + [\mathbf{M}_v])\{\ddot{\mathbf{v}}\} + ([\mathbf{C}] + [\mathbf{C}_v])\{\dot{\mathbf{v}}\} + ([\mathbf{K}] + [\mathbf{K}_v])\{\mathbf{v}\} = (\{\mathbf{f}_p\} + \{\mathbf{f}_v\}), \tag{13}$$

where $[\mathbf{M}]$, $[\mathbf{C}]$, and $[\mathbf{K}]$ are the mass, damping and stiffness matrices of the beam, respectively, $\{\mathbf{f}_p\}$ is the piezoelectric load vector and

$$[\mathbf{M}_v] = [\mathbf{0}] + m_v[\mathbf{N}]^{\mathrm{T}}[\mathbf{N}], \quad [\mathbf{C}_v] = [\mathbf{0}] + Vm_v([\mathbf{N}]^{\mathrm{T}}[\mathbf{N}'] - [\mathbf{N}']^{\mathrm{T}}[\mathbf{N}]),$$

$$[\mathbf{K}_v] = [\mathbf{0}] - V^2 m_v[\mathbf{N}']^{\mathrm{T}}[\mathbf{N}'], \quad \{\mathbf{f}_v\} = \{\mathbf{0}\} + m_v\mathbf{g}[\mathbf{N}]^{\mathrm{T}}. \tag{14}$$

In equation (14), it should be explicitly clear that the components of $[\mathbf{M}_v]$, $[\mathbf{C}_v]$, $[\mathbf{K}_v]$ and $\{\mathbf{f}_v\}$ matrices (14) are identically zero except those corresponding to the element under the moving mass. Moreover, $[\mathbf{C}_v]$ is a skew-symmetric matrix; i.e., $[\mathbf{C}_v] = -[\mathbf{C}_v]$. This clearly declares that the Coriolis term provides dynamic coupling rather than viscous damping.

For n finite elements, the dimension of each matrix in equation (13) is $(2n \times 2n)$. Details of these matrices are given in Appendix A. To simplify the presentation, equation (13) is expressed as

$$[\mathbf{M}_{eq}]\{\ddot{\mathbf{v}}\} + [\mathbf{C}_{eq}]\{\dot{\mathbf{v}}\} + [\mathbf{K}_{eq}]\{\mathbf{v}\} = \{\mathbf{f}_{eq}\} \tag{15}$$

with

$$[\mathbf{M}_{eq}] = ([\mathbf{M}] + [\mathbf{M}_v]), \quad [\mathbf{C}_{eq}] = ([\mathbf{C}] + [\mathbf{C}_v]),$$

$$[\mathbf{K}_{eq}] = ([\mathbf{K}] + [\mathbf{K}_v]), \quad \{\mathbf{f}_{eq}\} = (\{\mathbf{f}_p\} + \{\mathbf{f}_v\}). \tag{16}$$

2.4. STABILITY ANALYSIS

The considered beam is a time-varying system. The matrices given in equation (15) are periodic in time with period $\tau = L/V$. This period τ corresponds to the actual time needed for the moving mass to travel the beam length L at a constant speed V. An elegant theory to study the dynamics stability is suggested by Hsu [20; and Hsu and Cheng [23]] and is called the "impulsive parameter excitation theory". This theory requires the excitations to be represented by periodic heaviside step functions or Dirac delta functions [23]. The Hsu theory is very useful for multiple-degrees-of-freedom systems subjected to periodic parametric excitations of a general nature. The basic idea is to replace the continuously varying parametric excitation, within a period, by a sequence of a large number of impulses. This idea facilitates the computational effort for higher order systems. Adopting Hsu's theory, the homogeneous part of the second order system (15), first, is cast in a first order form

$$\{\dot{\mathbf{Z}}\} = [\mathbf{A}_d(t)]\{\mathbf{Z}\}, \tag{17}$$

with $\{\mathbf{Z}\} = \begin{pmatrix} \{\mathbf{v}\} \\ \{\dot{\mathbf{v}}\} \end{pmatrix}$ and

$$[\mathbf{A}_d(t)] = \begin{bmatrix} [\mathbf{0}] & [\mathbf{I}] \\ -[\mathbf{M}_{eq}]^{-1}[\mathbf{K}_{eq}] & -[\mathbf{M}_{eq}]^{-1}[\mathbf{C}_{eq}] \end{bmatrix}, \tag{18}$$

where $[\mathbf{A}_d(t)]$ is periodic of period τ. Now, each period is divided into K equal intervals with $[\mathbf{A}_d\,(t)]$ given by

$$[\mathbf{A}_d(t)] = \sum_{k=1}^{K} [\mathbf{A}_d^{(k)}] \sum_{m=-\infty}^{\infty} [\mathrm{H}(t - 2\pi m - t_{k-1}) - \mathrm{H}(t - 2\pi m - t_k)], \tag{19}$$

where

$$[\mathbf{A}_d^{(k)}] = [\mathbf{A}_d(t_k)] \quad \text{and} \quad t_k = \pi/2K\,(2k-1) \tag{20}$$

and H (t) is the heaviside step function. For this system, the growth matrix [**H**] as defined in reference [20] is

$$[\mathbf{H}] = \prod_{k=1}^{K} \mathrm{e}^{[\mathbf{A}_d^{(k)}](t_k - t_{k-1})}, \quad t_0 = 0. \tag{21}$$

Let the eigenvalues of [**H**] be denoted by λ. Depending on the values of $|\lambda|$, the stability of the system (in the Lyapunov sense) may be analyzed as:

(1) The system is asymptotically stable if, for all λ's, $|\lambda| < 1$.
(2) The system is unstable if at least one λ has $|\lambda| > 1$.
(3) The system is stable if some distinct λ's have $|\lambda| = 1$ and the rest of λ's have $|\lambda| < 1$.

The above analysis is based on the Floquet theory. More details of the previous theory can be found in references [20, 23].

In order to facilitate the computational effort, the bisection method is used to locate the stability boundary.

3. NUMERICAL EXAMPLES AND RESULTS

3.1. VERIFICATION EXAMPLE

As a first example, the dynamic stability, a uniform beam with simply supported ends is considered. The beam geometry and properties are the same as those considered by Nelson and Conover [15]. The beam is subjected to a moving mass that travels, at constant speed, from the left end to the right end. The stability map for this beam is obtained by using two finite elements and time intervals $K = 200$. This small number of finite elements was chosen in order to make comparisons with the results of Nelson and Conover in which two modes were used in the analysis. Figure 3 shows the transverse stability map obtained in the present study and by Nelson and Conover [15]. The two results agree quite well, emphasizing the accuracy of the impulsive parameter excitation theory and the developed finite element model.

3.2. STEPPED BEAM

A cantilever (C–F) beam, which is fixed at the left end and free at its right end, is considered. The beam comprises four steps with step factor $f = 1{\cdot}25$ and $L_s = L_n$ as shown in Figure 1. The steps are made of a material identical to those of the host beam. The beam is exposed to a moving mass travelling at constant speed from left to right. The internal damping a, is assumed to be 0·01; see Appendix A. The stability boundary of the stepped beam in the α–β plane is shown in Figure 4 for 7, 14 and 21 finite elements. It is clear that the results depend on the number of finite elements used in the analysis. This is especially true for α greater than 1·0 where high order modes dominate the behavior. For the considered number of finite elements, Figure 5 demonstrates that the number of finite elements has no pronounced influence on the results if α is less than 0·1. This indicates that, for very small values of α, the beam stability is dominated by the first mode. When α is less that 0·5, the results of 14 and 21 finite elements are essentially the same. Another presentation of the results is shown in Figure 6 whose abscissa is $\underline{\alpha} = \alpha/(1+\alpha)$ and ordinate is $\underline{\beta} = 2\pi\beta\alpha^{1/2}$.

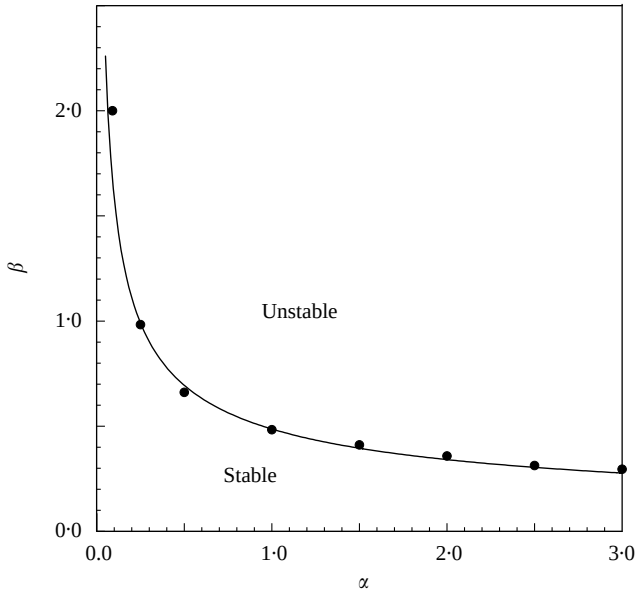

Figure 3. Stability map of a simply supported beam: ——, present results; ●, results from reference [15].

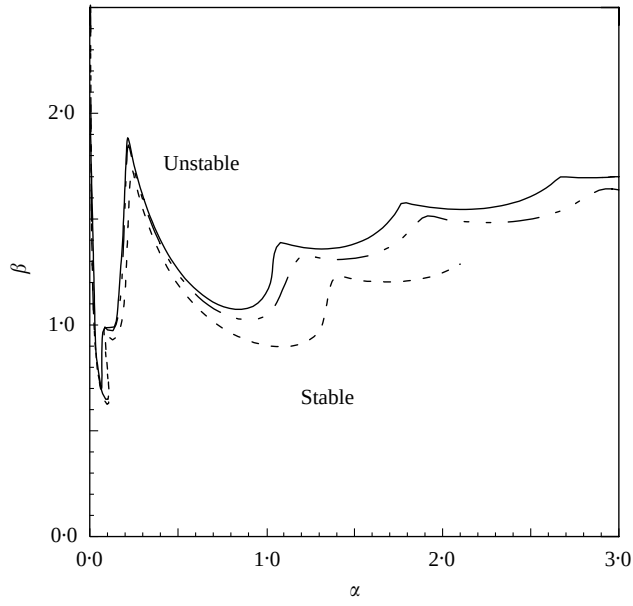

Figure 4. Stability map of a four steps beam for (- - -) 7, (— –) 14, and (——) 21 finite elements (F.E.).

Obviously, this presentation shows the effect of the dominant modes on the beam dynamic stability for various values of $\underline{\alpha}$. Note that this presentation is very common in the community of fluid–structure interactions [17]. If $\underline{\alpha}$ is less than 0·08, the beam becomes unstable by the first mode. For higher values such that $0{\cdot}08 < \underline{\alpha} < 0{\cdot}2$, the second mode becomes more prominent and for $0{\cdot}2 < \underline{\alpha} < 0{\cdot}6$, the third cantilever mode becomes apparent. High order modes become very effective when the values of $\underline{\alpha}$ increase. The jumps in the stability boundary indicate the appearance of higher dominating modes.

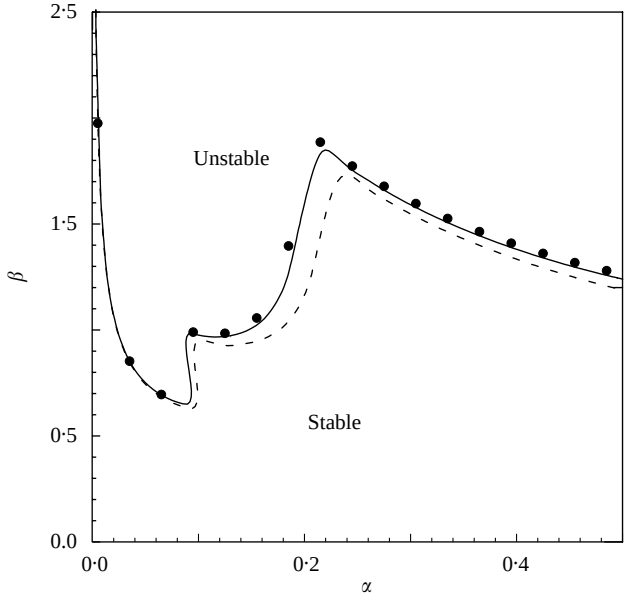

Figure 5. Stability map of four-stepped clamped–free beam: - - - -, 7 F.E.; ——, 14 F.E.; ●, 21 F.E.

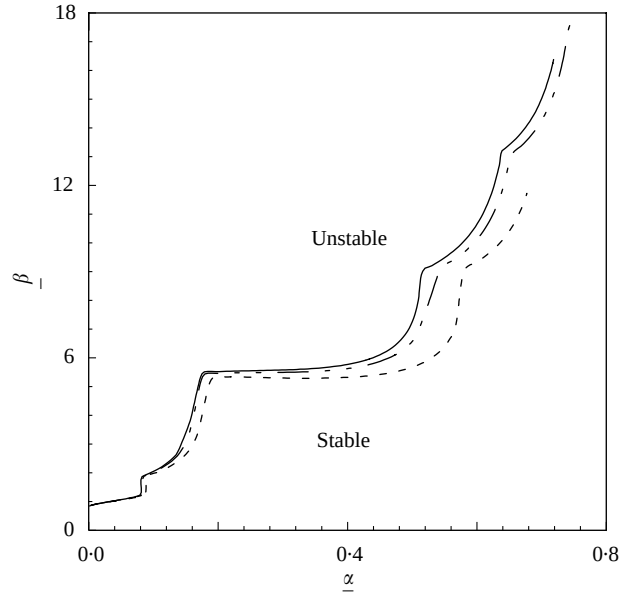

Figure 6. Another presentation of the stability map of four steps beam: - - -, 7 F.E.; — –, 14 F.E. and ———, 21 F.E.

3.3. UNIFORM VERSUS STEPPED BEAM

In this case, the dynamic stability of cantilever beams with uniform and non-uniform cross-section is investigated. To ensure accuracy, 21 finite elements are used in the analysis. The uniform beam has a hollow circular cross-section of inner diameter $D_i = 14$ mm and

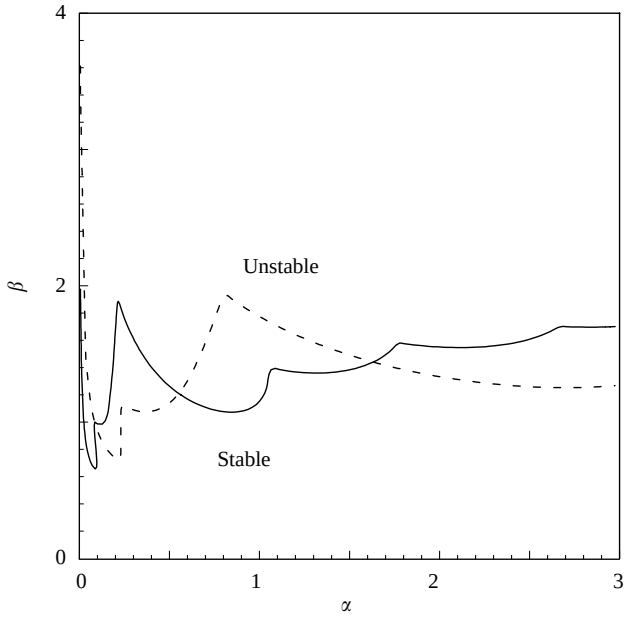

Figure 7. Stability map of uniform and four-stepped C–F beam: ——, 4 steps; - - -, uniform.

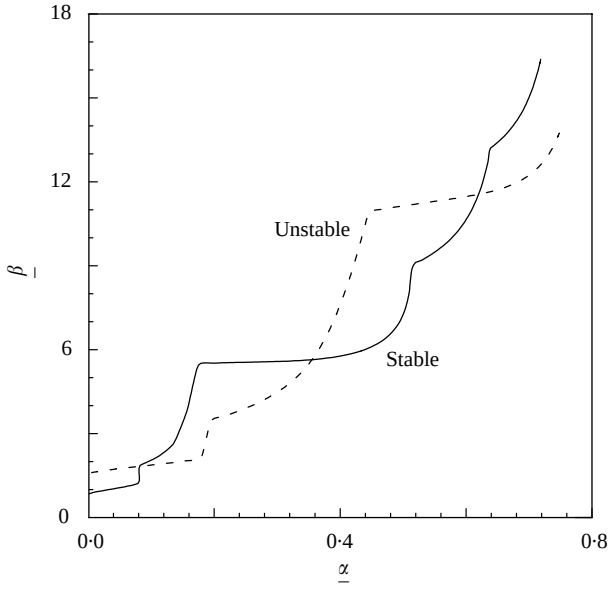

Figure 8. Another presentation of the stability map of uniform and four steps beam. ——, 4 steps; – – –, uniform.

outer diameter $D_o = 16$ mm. The non-uniform beam contains four steps and has a hollow circular cross-section of inner diameter D_i. Furthermore, the outer diameter of the stepped regions is D_o and the remaining regions have diameters of $0{\cdot}8D_o$. Figures 7 and 8 show the stability maps of uniform and stepped beam in two different planes; namely, the α–β plane and the $\underline{\alpha}$–$\underline{\beta}$ plane. When $\alpha < 0{\cdot}1$ or ($\underline{\alpha} < 0{\cdot}08$), the stepped beam loses stability at β (or $\underline{\beta}$) smaller than those of a uniform beam. This is because the uniform beam stiffness is higher

than that of the stepped beam. In the range $0{\cdot}1 < \alpha < 0{\cdot}55$ or ($0{\cdot}08 < \underline{\alpha} < 0{\cdot}36$), the stepped beam has better stability characteristics than that of a uniform cross-section. For the considered ranges, the stability of the stepped beam is governed by a number of modes that are greater than those of a uniform beam. This is clearly shown by the number of jumps in the stability maps.

3.4. STEPPED PIEZOELECTRIC BEAM

In this case, the dynamic stability of a cantilever beam under a moving mass travelling at constant speed from left to right end is investigated. The beam comprises four PZT5H piezoelectric steps with step factor $f = 1{\cdot}25$ and $L_s = L_n$ as shown in Figure 1. Twenty-one finite elements are used in the analysis. The host beam has a hollow circular cross-section of inner diameter $D_i = 14\,\text{mm}$ and outer diameter $D_o = 16\,\text{mm}$. The piezoelectric steps are perfectly attached to the host beam. Figure 2a depicts the beam cross-section at a step region. Each piezoelectric step is supplied with actuation voltage such that the piezoelectric moment is related to the second derivative of the deflection at the step ends and is given by

$$M_y^p = gain(w''_{right\ end} - w''_{left\ end}).$$

Figures 9 and 10 show the stability maps of uniform and stepped (gain = 0) piezoelectric beam in two different planes; namely, the α–β plane and the $\underline{\alpha}$–$\underline{\beta}$ plane. When $\alpha < 0{\cdot}1$ or ($\underline{\alpha} < 0{\cdot}08$), the uniform beam loses stability at β (or $\underline{\beta}$) smaller than those of a stepped beam. This is because, in this case, the stepped beam is stiffer than a uniform beam. The figures also show the stability maps of beams controlled by piezoelectric steps. It is clear that the beam stability can be significantly improved by the piezoelectric steps. And, the larger the control gain the better the stability characteristics. In the range $0{\cdot}8 < \alpha < 1{\cdot}8$ or ($0{\cdot}4 < \underline{\alpha} < 0{\cdot}6$), the piezoelectric actuators have an insignificant effect on the stability characteristics.

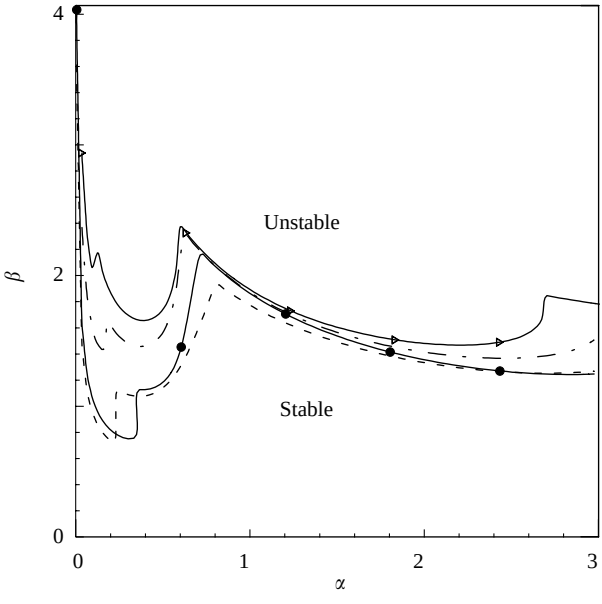

Figure 9. Stability map of uniform and four steps piezoelectric C–F beam: – – –, unform; –●–, gain = 0; — – —, gain = 42; –▷–, gains = 82.

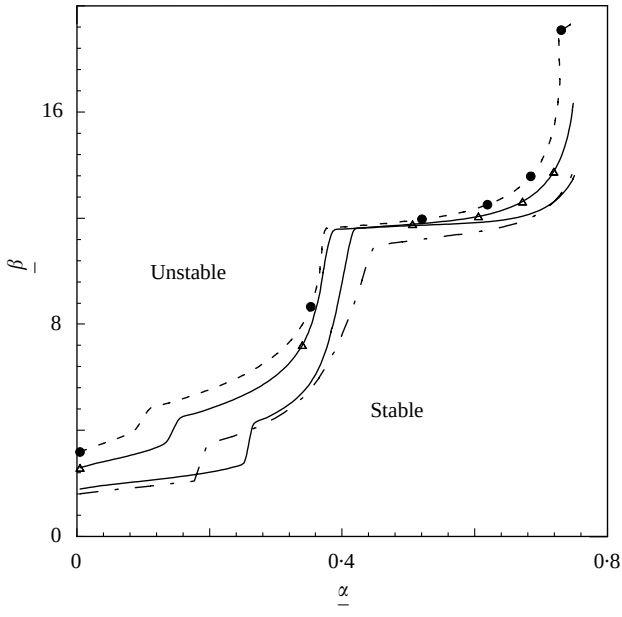

Figure 10. Another presentation of the stability map of uniform and four steps piezoelectric C–F beam: – – –, uniform beam; ——, gain = 0; –△–, gain = 42; – –●– –, gain = 84.

4. CONCLUSIONS

The equations of motion of a stepped beam subjected to moving mass are formulated and presented in two forms; namely, distributed parameter form and finite element form. Unlike the previous studies, which employ Galerkin's method along with Mathieu–Hill method, the authors employed finite element techniques along with impulsive parametric excitation to investigate the dynamic stability of the beam. The stability analysis of the present study is verified by examining a simply supported beam and comparing the results with the previously reported results in the literature. Stability maps are obtained for clamped–free stepped beam and for clamped–free uniform beam. For large ratios of moving mass to beam mass, more finite elements are needed to accurately identify the stability boundaries. It is also found that the stability of certain beam modes can be improved by using the stepped beam configuration. It is shown that a better stability characteristic can be obtained by using piezoelectric steps. The analysis developed in the present study is being extended to investigate the dynamic stability of beams carrying a series of mass particles. Furthermore, stability analysis of beams with periodic piezoelectric and/or viscoelastic steps is a natural extension of the present work.

REFERENCES

1. S. A. Siddiqui, M. F. Golnaraghi and G. R. Heppler 2000 *Journal of Sounds and Vibration* **229**, 1023–1055. Dynamics of flexible beam carrying a moving mass using perturbation, numerical and time–frequency analysis techniques.
2. M. Abu Hilal and H. S. Zibdeh 2000 *Journal of Sound and Vibration* **229**, 377–388. Vibration analysis of beams with general boundary conditions traversed by a moving force.
3. M. Ichikawa, Y. Miyakawa and A. Matsuda 2000 *Journal of Sound and Vibration* **230**, 493–506. Vibration analysis of the continuous beam subjected to a moving mass.
4. M. A. Foda and Z. Abduljabbar 1998 *Journal of Sound and Vibration* **210**, 295–306. A dynamic green function formulation for the response of a beam structure to a moving mass.

5. E. ESMAILZADEH, and M. GHORASHI 1995 *Journal of Sound and Vibration* **184**, 9–17. Vibration analysis of beams traversed by uniform partially distributed moving masses.
6. J. R. RIEKER and M. W. TRETHEWEY 1999 *Mechanical Systems and Signal Processing* **13**, 31–51. Finite element analysis of an elastic beam structure subjected to a moving distributed mass train.
7. D. Y. ZHENG, Y. K. CHEUNG, F. T. K. AU and Y. S. CHENG 1998 *Journal of Sound and Vibration* **212**, 455–467. Vibration of multi-span non-uniform beams under moving loads by using modified beam vibration functions.
8. J. R. RIEKER, Y.-H. LIN and M. W. TRETHEWEY 1996 *Finite Elements in Analysis and Design* **21**, 129–144. Discretization consideration in moving load finite element beam models.
9. Y-H. LIN and M. W. TRETHEWEY, 1990 *Journal of Sound and Vibration* **136,** 323-342. Finite element analysis of elastic beams subjected to moving dynamic loads.
10. L, FRYBA 1972 *Vibration of Solids and Structures under Moving loads.* Groningen, The Netherlands: Noordhoff.
11. S. SAIGAL 1986 *American Society of Mechanical Engineers Journal of Applied Mechanics* **53**, 222–224. Dynamic behavior of beam structures carrying moving masses.
12. Y-H. LIN, M. W. TRETHEWEY, H. M. REED, J. D. SHAWLEY and S. J. SAGER 1990 *American Society of Mechanical Engineers Journal of Vibration and Acoustics* **112**, 355–365. Dynamic modeling and analysis of a high speed precision drilling machine.
13. R. KATZ, C. W. LEE, A. G. ULSOY and R. A. SCOTT 1987 *American Society of Mechanical Engineers Journal of Vibration, Acoustics, Stress, and Reliability in Design* **109**, 361–365. Dynamic stability and response of a beam subjected to a deflection dependent moving load.
14. G. A. BENEDETTI 1974 *American Society of Mechanical Engineers Journal of Applied Mechanics* **41**, 1069–1071. Dynamic stability of a beam loaded by a sequence of moving mass particles.
15. H. D. NELSON and R. A. CONOVER 1971 *American Society of Mechanical Engineers Journal of Applied Mechanics* **38**, 1003–1006. Dynamic stability of a beam carrying moving masses.
16. G. W. HOUSNER 1965 *American Society of Mechanical Engineers Journal of Applied Mechanics* **74**, 351–358. Bending vibrations of a pipe line containing flowing fluid.
17. R. W. GREGORY and M. P. PAIDOUSSIS 1966a *Proceedings of the Royal Society* (*London*) **A 293**, 512–527. Unstable oscillation of tubular cantilevers conveying fluid. I. Theory.
18. R. W. GREGORY and M. P. PAIDOUSSIS 1966b *Proceedings of the Royal Society* (*London*) **A 293**, 528–542.Unstable oscillation of tubular cantilevers conveying fluid. II. Experiments.
19. V. V. BOLOTIN 1964 *The Dynamic Stability of Elastic System.* San Francisco: Holden-Day.
20. C. S. HSU 1972 *American Society of Mechanical Engineers Journal of Applied Mechanics* **39**, 551–558. Impulsive parametric excitation: Theory.
21. D. B. MCIVER 1973 *Journal of Engineering Mathematics* **7**(3) 249–261. Hamilton's principle for systems of changing mass.
22. R. W. CLOUGH and J. PENZIEN 1975 *Dynamics of Structures*, New York: McGraw-Hill.
23. C. S. HSU and W-H. CHENG 1973 *American Society of Mechanical Engineers Journal of Applied Mechanics* **40**, 78–86. Applications of the theory of impulsive parametric excitation and new treatments of general parametric excitation problems.

APPENDIX A: BEAM MATRICES

The beam matrices in the finite element model, given by equation (13), are defined as

$$\textit{Mass}: [\mathbf{M}] = \int_0^L \rho A[\mathbf{N}]^{\mathrm{T}}[\mathbf{N}]\mathrm{d}x,$$

$$\textit{Stiffness}: [\mathbf{K}] = \int_0^L EI[\mathbf{N}'']^{\mathrm{T}}[\mathbf{N}'']\mathrm{d}x,$$

$$\textit{Internal damping}: [\mathbf{C}] = \int_0^L \eta I[\mathbf{N}'']^{\mathrm{T}}[\mathbf{N}'']\mathrm{d}x,$$

If η is chosen such that $\eta = a\,E$ (i.e., a is a small and positive constant), then $[\mathbf{C}] = a[\mathbf{K}]$.

$$\textit{Piezoelectric load}: \{\mathbf{f}_p\} = -\int_0^L M_y^p[\mathbf{N}'']^{\mathrm{T}}\mathrm{d}x.$$

APPENDIX B. NOMENCLATURE

A	cross-sectional area
$[\mathbf{A}_d]$	system matrix (in equation (18))
a	small positive constant (in equation (A.4))
$[\mathbf{C}]$	beam damping matrix
$[\mathbf{C}_v]$	skew matrix due to moving mass
D	outer diameter of the beam
D_i	inner diameter of the beam
E	beam Young's modulus
f	step factor (see Figure 1)
$\{\mathbf{f}_p\}$	piezoelectric load vector
$\{\mathbf{f}_v\}$	load vector due to moving mass
$\mathbf{g}$	acceleration due to gravity
$[\mathbf{H}]$	growth matrix (in equation (21))
$[\mathbf{H}(t)]$	Heaviside step function
H_T	constant term (in equation (7))
h	finite element length
I	beam moment of inertia
$[\mathbf{K}]$	beam stiffness matrix
$[\mathbf{K}_v]$	stiffness matrix due to moving mass
L	beam length
$[\mathbf{M}]$	beam mass matrix
$[\mathbf{M}_v]$	mass matrix due to moving mass
M_y^p	y-component of the piezoelectric moment
M^p	piezoelectric resultant moment
m_v	mass of the moving mass
N_i	shape functions
T	total kinetic energy of the beam system
t	time
T_b	kinetic energy of the elastic beam
T_m	kinetic energy of the moving mass
U	total strain energy of the beam system
u	axial displacement of the beam
V	speed of moving mass
v_i	nodal d.o.f.
v_x	x-component of the absolute velocity of moving mass
v_z	z-component of the absolute velocity of moving mass
W_{nc}	work of non-conservative loads
w	transverse displacement of the beam

Greek letters

α	dimensionless mass ratio ($= m_v/\rho AL$)
β	dimensionless speed ratio ($= VL/2\pi\sqrt{\rho A/EI}$)
$\underline{\alpha}$	$\alpha/(1+\alpha) = m_v/(\rho AL + m_v)$
$\underline{\beta}$	$= 2\pi\beta\alpha^{1/2} = VL\sqrt{m_v/EIL}$
δ	first variation
$[\delta(x)]$	Dirac delta function
ε_x^p	axial piezoelectric strain
η	damping coefficient of the beam material
λ	eigenvalue of the growth matrix H
ρ	mass density of the beam
τ	time period

Superscripts

T	transpose
$(\bullet)'$	$= \partial(\bullet)/\partial x$
$(\dot{\bullet})$	$= \partial(\bullet)/\partial t$